Quantum Stochasticity Effects on Angular Distributions in Electron-Beam Collision with Laser Pulse*

Ming Zi,[1] Yanyun Ma,[2,3,†] Xiaohu Yang,[2] Guobo Zhang,[2] Jianxun Liu,[4] Wei Xiong,[1] Tong Wu,[2] Yanqin Deng,[2] and Fuqiu Shao[1]

[1] *College of Science, National University of Defense Technology, Changsha 410073, China*
[2] *College of Advanced Interdisciplinary Studies, National University of Defense Technology, Changsha 410073, China*
[3] *Collaborative Innovation Center of IFSA (CICIFSA), Shanghai Jiao Tong University, Shanghai 200240, China*
[4] *Early Warning Academy, Wuhan 430019, China*

This study investigates the influence of quantum stochasticity on angular distributions of electrons and positrons generated during the interaction between a laser wakefield acceleration (LWFA) electron beam and ultra-intense laser pulses. Distinct features are identified in the angular distributions of both the electron beam and high-energy photons, offering a crucial diagnostic tool for probing strong-field QED phenomena. While the kinetics of electrons in the laser field are typically governed by the deterministic Landau-Lifshitz (LL) equation. Furthermore, quantum stochastic effects(QSE) substantially affects the angular evolution and energy spectrum of the electron beam exhibit different behaviors. For high energy photons, the impact of QSE on the average divergence evolution due to lepton pair production. The detection and analysis of these characteristic signals provide crucial empirical insights for advancing LWFA-driven all-optical radiation sources and optimizing lepton-pair production techniques.

Keywords: Nonlinear Compton Scattering,Nonlinear Breit-Wheeler,Angular Distribution,LWFA-electrons,Strong-Field QED

I. INTRODUCTION

Highly energetic laser-plasma interactions have opened up unprecedented avenues for exploring the Quantum Electrodynamics (QED) under extreme conditions[1–3]. These interactions intricately couple the momentum distribution of particles with electromagnetic fields, leading to a wide range of novel physical phenomena[4–7]. With the continuous advancement of electron beam energies and the achievement of ultra-intense laser fields, it becomes imperative to incorporate radiation reaction (RR) effects and explore the implications of entering the QED-dominated regime. This regime is characterized by distinctive quantum phenomena, including stochastic photon emission, electron-positron pair production, spectral hard cutoffs, and quantum straggling effects [8–11]. When an electron beam interacts with an ultra-intense laser pulse, the final electron energy and deflection angle are determined by the initial electron energy and laser intensity [12]. The transition between classical RR and quantum radiation reaction (QRR) can be realized through the configuration of a laser wakefield acceleration (LWFA) electron beam colliding with an ultra-intense laser pulse [13–15]. In the QRR regime, the investigation of deflection angles serves as a crucial diagnostic tool for unraveling the complexities of strong-field QED effects [16]. Precise measurements of particle angular distributions provide valuable insights into the intricate interplay between intense laser fields and charged particles, thereby advancing our understanding of non-linear QED fundamentals. The pioneering observation of Breit-Wheeler pair production in SLAC's E144 experiment, which utilized a laser pulse with intensity $10^{18}\ \mathrm{W/cm^2}$ interacting with a $46\mathrm{GeV}$ electron beam from a linear accelerator, marked a significant milestone in strong-field QED research [17]. In recent years, laser-driven particle accelerators have attracted considerable attention due to their potential to revolutionize accelerator physics, particularly through their capability to generate high-energy electron beams. Among these, LWFA has emerged as a promising technique for charged particle acceleration, achieving remarkable progress in experimental demonstrations [18–20]. This technique enables the acceleration of electron beams to multi-GeV energies over centimeter-scale distances while maintaining exceptionally small divergence angles [19–21]. The development of all-optical schemes, which utilize LWFA electron beams colliding with intense lasers to produce high-energy photons, has provided experimental evidence of quantum effects in these interactions [9, 23]. Notably, angular distributions exhibit distinct features that serve as signatures of QRR and RR. Comparative studies employing Monte Carlo simulations, classical Landau-Lifshitz models, and modified Landau-Lifshitz formulations have systematically investigated the characteristics of electron angular distributions [24, 25].

The investigation of angular distributions in high-intensity laser-electron interactions represents a crucial approach for quantifying and understanding Quantum Electrodynamics (QED) phenomena under extreme laboratory conditions. When electrons interact with intense laser pulses, where the laser field acts as a target, they undergo quantum photon emissions that significantly alter their trajectories. These trajectory perturbations, characterized by measurable deflection angles, provide observable signatures of the intrinsic quantum stochasticity inherent in particle emission processes during all-optical experiments at modern laboratory laser intensities. Within the QED regime, electrons exhibit oscillatory motion without substantial energy loss - a phenomenon that

* Supported by the National Natural Science Foundation of China (Grant Nos. 11975308,11805278,11775305,12005297,and 12075306)
† Corresponding author, Yanyun Ma, yanyunma@126.com

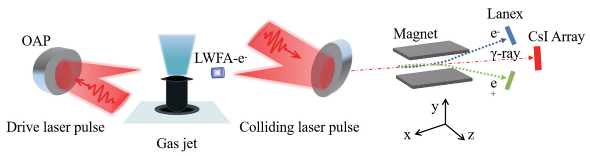

Fig. 1. Schematic diagram of the all-optical configuration for a laser wakefield acceleration (LWFA) electron beam interacting with a counter-propagating laser pulse. The illustration depicts two distinct phases: (a) the generation of the LWFA electron beam through the interaction of a driving laser pulse with a plasma target, and (b) the collision stage, where the accelerated electron beam interacts with the intense laser pulse, triggering nonlinear Compton scattering (nlCS) and nonlinear Breit-Wheeler (nlBW) pair production processes.

cannot be explained by classical electrodynamics but rather emerges as a direct manifestation of quantum stochasticity effects (QSE). The configuration of a laser wakefield acceleration (LWFA) electron beam $\left(\gamma_e \sim 10^3 \gg a_0\right)$ colliding with an ultra-intense laser pulse offers distinct advantages over direct laser-plasma interactions, as illustrated in Fig. 2. A critical aspect of this study involves the detailed analysis of divergence angles for both the LWFA electron beam and emitted photons, taking into account the influence of QSE and the Lorentz force exerted by the laser field.

The structure of this paper is organized as follows. Section 2 examines the kinetic evolution of charged particles in the context of strong-field QED, providing a comprehensive theoretical foundation through the derivation of formulas governing the differential emission rates for nonlinear Compton scattering (nlCS) and nonlinear Breit-Wheeler (nlBW) processes. Section 3 focuses on the effects of quantum stochasticity on the angular distributions of both the LWFA electron beam and nlCS photons during their interaction with the laser field. This analysis reveals the complex interplay between particle dynamics and quantum processes under extreme conditions, highlighting distinctive structural features of quantum interactions. Finally, Section 4 summarizes the key findings and presents conclusions drawn from the study.

II. QED EMISSION

Theoretical and numerical investigations of quantum emission processes typically rely on the assumption that the formation length (time) is significantly smaller than the characteristic spatial (temporal) scale of the laser field [26, 27]. The mean free path for electrons and photons are on the order of the Compton wavelength $\lambda_c \sim 1/m_e$ for $\alpha\eta^{2/3} \sim 1$[11]. At this scale, the classical description of particle motion becomes inadequate. Radiative correction calculations suggest that loop corrections in strong-field QED may increase with the energy scale. According to the "Ritus-Narozhny conjecture", the semi-perturbative expansion of strong field QED break down when $\alpha\eta^{2/3} \sim 1$ [28]. In our configuration, the Lorentz quantum invariant remains significant below this critical limit. By incorporating quantum corrections into the Landau-Lifshitz (LL) equation, the momentum evolution of a relativistic charged particle can be described by the modified equation [15]:

$$\frac{d\mathbf{p}}{dt} = q(\mathbf{E} + \mathbf{u} \times \mathbf{B}) - \frac{P_q \mathbf{u}}{\mathbf{u}^2} \tag{1}$$

where P_q represents the quantum-corrected radiation power, expressed as $P_q = P_0 g(\eta) \alpha^2 \eta^2$.Here P_0 denotes the classical Larmor radiation power, and $g(\eta) = \left[1 + 4.8(1+\eta)\ln(1+1.7\eta) + 2.44\eta^2\right]^{-2/3}$ is the quantum correction function[29]. The electric and magnetic fields are represented by $\mathbf{E}$ and $\mathbf{B}$, respectively, while $\mathbf{u}$ is the normalized velocity $\mathbf{p}/(\gamma mc)$. Lorentz quantum invariant parameters are defined as: $\eta = \left(e/m_e^3\right)|F_{\mu v} p^v|$.and $\chi = \left(e/m_e^3\right)|F_{\mu v} k^v|$, where $F_{\mu v} = \partial_\mu A_v - \partial_v A_\mu$ is the electromagnetic field tensor, p^v is electron 4-momentum $(\varepsilon/c, \mathbf{p})$, k^v is photon 4-wave vector $(\omega/c, \mathbf{k})$ [30]. For electrons in the laser field treated as seed electrons, the Lorentz quantum invariant is given by $\eta_{\mathrm{L}} = \gamma E \sin\theta / E_S$, where E_S is Schwinger field, $\gamma_{\mathrm{L}} \approx \sqrt{1 + a^2/2}$ is the Lorentz factor for electrons accelerated by a linearly polarized laser pulse in the zero-momentum frame, and θ represents the angle between the electric field and electron momentum [31]. In the configuration of a LWFA electron beam head-on collision with an ultra-intense laser pulse, the invariant becomes $\eta_{\mathrm{d}} = 2\gamma_{\mathrm{LWFA}} E/E_S$. Here γ_{LWFA} can significantly exceed γ_{L} due to the intensity of driving laser pulse in our configuration, as illustrated in Fig. 2.

The local differential radiation rate probability for an electron emitting one-photon through nonlinear Compton scattering is given by[28, 32, 33]:

$$\frac{d^2 N_{ph}}{dt d\omega} = \frac{\alpha_f}{\sqrt{3}\pi\tau_c\gamma_e^2}\left\{\left(2 + \frac{3}{2}\chi\delta\right) K_{2/3}(\delta) - \int_\delta^\infty K_{1/3}(s) ds\right\} \tag{2}$$

where $\delta = 2\chi/3\eta(\eta - \chi), \tau_c = 1/m$ is the Compton wavelength, and $K_v(x)$ denotes the modified Bessel function of the second kind. For the decay of a high-energy photon into lepton pairs (e^+e^-) in an ultra-intense laser pulse, the differential rate probability is given by [28, 34–36]:

$$\frac{d^2 N_p}{dt d\gamma_p} = \frac{\alpha_f m^3}{\sqrt{3}\pi\omega^2}\left\{\left(\frac{3}{2}\chi\rho - 2\right) K_{2/3}(\rho) - \int_\rho^\infty K_{1/3}(s) ds\right\} \tag{3}$$

where $\rho = 2\chi/3\eta_p\left(\chi - \eta_p\right)$, with η_p and γ_p representing the Lorentz invariant and Lorentz factor of the positron created in the nonlinear Breit-Wheeler (nlBW) process, respectively.

The enhancement of Lorentz invariants suggests that, at identical laser intensities, the yield of photons and electron-positron pairs from LWFA electron beam-laser collisions can surpass that from direct laser-accelerated electrons. The superior energy and momentum characteristics of LWFA electrons facilitate the attainment of threshold conditions for QED processes. Well-collimated LWFA electron beams further amplify the Lorentz invariant, thereby increasing the probability of QED processes and potentially generating more high-energy photons and electron-positron pairs under equivalent laser intensities. This advantage underscores the potential of

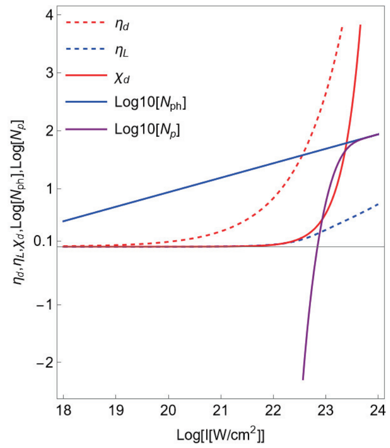

Fig. 2. Evolution of Lorentz quantum invariants in a single laser cycle for an electron with ($\gamma_{\mathrm{LWFA}} = 2000$). The Lorentz quantum invariant η_{d}, χ_{d} is invariant the photon|experienced in the laser field, and η_{L} represents the invariant of the electron accelerated by the linearly polarized laser pulse, and N_{p} and $N_{\mathrm{p}h}$ indicate the number of pair and photon produced in one laser period by a head-on colliding electron.

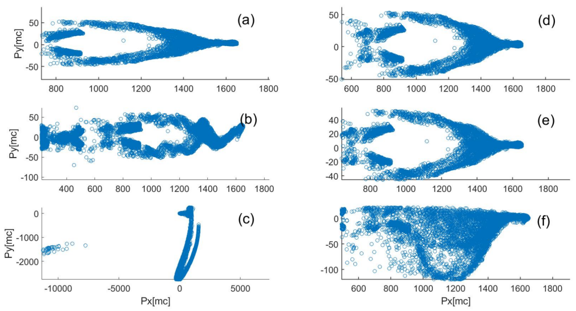

Fig. 3. Comparing of electron kinetic evolution without-QED effects (a,b,c) and with-QED effects (d,e,f) during collision with a planar laser pulse (10^{21} W). The simulation parameters for the LWFA electron beam are detailed in Section 3. The divergence angle evolution is shown: initial state before collision (a,d), after 3 laser cycles (b,e), and after 4 laser cycles (c,f).

LWFA technology in advanced photon and positron generation research. Detailed calculations and analyses based on specific experimental parameters and theoretical models are required to fully characterize the physical properties of the produced photons and positrons.

To account for realistic experimental conditions, including the spatial and energy spectrum structure of the LWFA electron beam and the spatiotemporal characteristics of the colliding laser, large-scale particle-in-cell (PIC) simulations are essential. Figure 3(e) demonstrates that the inclusion of QED effects results in relatively stable divergence angles, contrasting with Figure 3(b). In Figure 3(f), the electron divergence angle is an order of magnitude smaller than in Figure 3(c). When the transverse momentum component exceeds the longitudinal momentum, the angular distribution develops a double-peak structure, typically indicative of a ring-like pattern in head-on collisions due to the interplay between Lorentz forces and radiation reaction [25]. In regimes where quantum stochasticity effects (QSE) dominate, the energy of the colliding electron beam is primarily converted into photons and positrons. The Lorentz force of the laser pulse then governs the collective electron behavior, leading to the characteristic ring structure in the angular distribution. In the Lorentz-force-dominated regime, transverse momentum is amplified within the laser field, potentially resulting in angular distribution evolution exhibiting laser-frequency-dependent structures. Experimental observations have confirmed that electron angular distributions exhibit QSE signatures, confirming photon production through the nlCS process. The characteristic evolution of particle divergence angles serves as a diagnostic signature for both nlCS and nlBW processes.

III. EVOLUTION OF ANGULAR DISTRIBUTION

Given the inherent symmetry of linear laser fields along the propagation direction (x-axis), our analysis focuses on the transverse (y-direction) asymmetry in deflection angles. In linearly polarized laser fields, the z-component of electron momentum simplifies our investigation by enabling us to concentrate on transverse dynamics. To effectively examine the influence of quantum stochasticity effects (QSE) on deflection angles, we employ an optimized two-dimensional (2D) simulation framework. This dimensional reduction strategy maintains physical fidelity while significantly reducing computational complexity. Our simulations investigate the interaction between LWFA electrons and the laser field in the xy-plane, incorporating only the essential forces and processes governing transverse dynamics. To enhance electron energy output, we implement a density jump target strategy, which, while reducing beam charge, facilitates the generation of higher energy electrons. Consequently, the LWFA electron beam achieves the cut-off energy shown in Fig. 6(d), with the corresponding angular distribution illustrated in Fig. 5(a).

The simulation employs particle-in-cell (PIC) numerical techniques, where each simulated particle represents a 'macro-particle' characterized by specific density, weighting, and momentum parameters to accurately model collective electron behavior while maintaining computational efficiency [37–39]. Figure 4(b) reveals that the photon distribution comprises two distinct components. The central region consists of highly collimated photons generated by the LWFA electron beam, which subsequently produce positrons through the nonlinear Breit-Wheeler (nlBW) process, as shown in Fig. 4(c). The transverse photon distribution exhibits periodicity corresponding to the laser wavelength. During the LWFA electron beam-laser collision, longitudinal momentum is transferred to photons within approximately six laser periods. Subsequently, electron dynamics become dominated by lateral oscillations in the laser field, producing photons that rarely generate nlBW positrons. Low-energy electrons primarily respond to electromagnetic forces, exhibiting collective displacement that can be described classically.

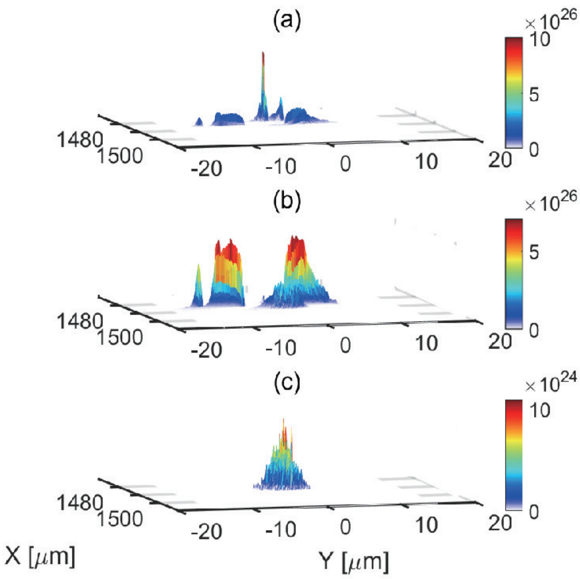

Fig. 4. Density distribution of electrons (a), photons (b), and positrons (c) at $t = 5/\omega_{\mathrm{L}}$ following the collision of an LWFA electron beam with a 10^{23} $\mathrm{W/cm^2}$ linearly polarized (y-direction) planar laser pulse.

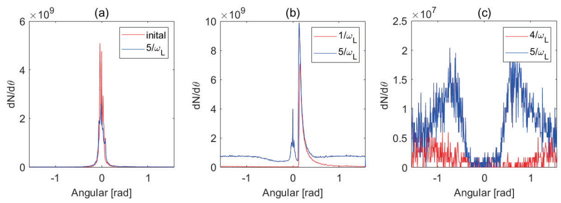

Fig. 5. Angular distributions of (a) electrons, (b) photons, and (c) positrons following the collision of an LWFA electron beam with a 10^{23} $\mathrm{W/cm^2}$ laser pulse.

The angular distribution of the LWFA electron beam evolves significantly after $t = 5/\omega_{\mathrm{L}}$, demonstrating the laser field's impact on spatial distribution and propagation direction, as shown in Fig. 5(a). Figure 5(b) contrasts the angular distribution of photons at production initiation and after $t = 5/\omega_{\mathrm{L}}$ interaction. As massless gauge bosons, photon angular momentum changes exclusively through nlCS involving LWFA electron beams and nlBW processes in the laser field, making QSE effects particularly evident in photon angular momentum distribution studies. Figure 5(c) illustrates that positron production in our configuration occurs without significant cascade effects [40]. Positrons are generated with relatively low energies and undergo transverse acceleration in the plane-wave laser field, resulting in a characteristic double-peak structure that reflects classical deterministic dynamics. This behavior underscores the importance of considering colliding laser pulse duration and particle extraction methods in future research.

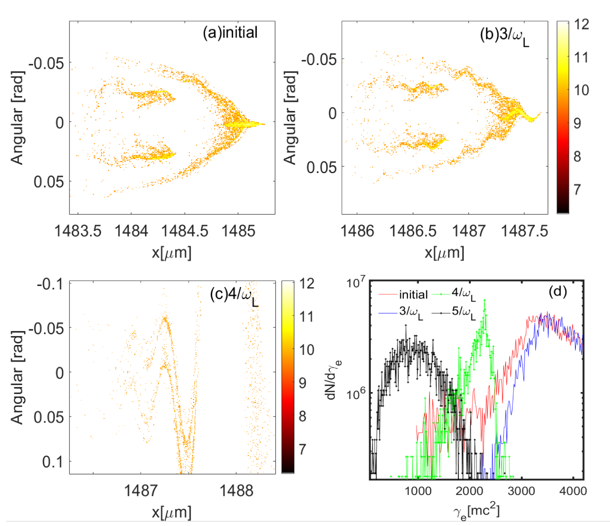

Fig. 6. Evolution of electron angular distribution: (a) initial LWFA electron beam, (b) after $t = 3/\omega_{\mathrm{L}}$ collision with 10^{23} $\mathrm{W/cm^2}$ at (b), and (c) after $4/\omega_{\mathrm{L}}$. The color scale represents $\log_{10}\left[\mathrm{d}^2 N_e/\mathrm{d}\theta \mathrm{d}x\right]$ versus deflection angles $\theta = \arctan\left(p_y/p_x\right)$ and x-position. (d) Energy spectrum evolution at different interaction times.

A. Electron Beam Angular Divergence Evolution

The energy transfer mechanism from high-energy electrons to photons is governed by the Lorentz invariant discussed in Section 2. High-energy electrons act as seeds for additional perpendicular acceleration in the laser field, producing more photons. However, photons produced immediately after collision typically lack sufficient energy for direct positron production in the same laser field. Instead, positron generation primarily results from high-energy photons produced during the initial LWFA electron beam-laser interaction. These photons in the beam-head region possess adequate energy to initiate e^+e^- pair production through the nlBW process, requiring specific photon energy thresholds related to the invariant χ, as illustrated in Fig.2.

The energy spectrum evolution in Fig. 6(d) reveals that after $3/\omega_L$ (blue line), the high-energy region nearly coincides with the pre-collision LWFA electron spectrum (red line), contradicting Landau-Lifshitz deterministic predictions and demonstrating QSE signatures. Electron angular distribution further confirms QSE presence, as evidenced by comparing Fig. 6(a) and (b). By $t = 4/\omega_L$ (green dotted line), high-energy LWFA electrons have predominantly converted to photons through nlCS, largely completing subsequent nlBW processes. While electrons continue interacting with the laser pulse, producing additional nlCS photons, these photons do not contribute significantly to further nlBW processes, as discussed in Section 3.2. The energy spectrum evolution from $t = 4/\omega_L$ (green dotted line) to $5/\omega_L$ (black dotted line) in Fig. 6(d) demonstrates laser field dominance over QSE effects. This evolution incorporates both diffusion and drift components, reflecting spectral shifts and shape changes. Our PIC simulations treat nlCS and nlBW processes separately,

excluding cascade effects [37]. The Fokker-Planck equation adequately describes electron spectrum evolution, derived by truncating the Boltzmann equation source term into two components. In natural units, the electron energy evolution follows: $d\gamma(t) = -S(\eta)dt + \sqrt{R(\eta,\gamma)}dW(t)$ in nature unit[14, 41], where $\mathrm{W(t)}$ represents the wiener stochastic process, $S(\eta) \approx 1.5\alpha m^2\eta^2$ and $R(\eta,\gamma) \approx 1.3\alpha m^3\gamma\eta^3$ is the drift coefficient and diffusion coefficient, respectively. Figure 6(d) identifies distinct regimes: QSE dominance before $4/\omega_{\mathrm{L}}$, and the the $S(\eta)$ and $R(\eta,\gamma)$ determinate the evolution of the energy spectrum.

B. Photons Average Divergence Evolution

To accurately identify the characteristic signatures of quantum stochasticity effects (QSE) on the nonlinear Breit-Wheeler (nlBW) process, we focus on analyzing the evolution of the average divergence angle of photons in a plane-wave field, taking advantage of their charge neutrality in the laser field. The observed asymmetry in deflection angles along the y-direction is directly linked to the complex interplay of QSE. We define the average divergence angle as follows:

$$< \theta >= \arctan\left(\frac{\sum_{\mathrm{i}=1}^{N}\frac{\mathrm{w_i * k_y}}{\mathrm{k_x}}}{\sum_{\mathrm{i}=1}^{N}\mathrm{w_i}}\right) \tag{4}$$

where $\mathrm{w_i}$ is the weight factor of the i-th the macroparticle of the N macroparticles. In a laser field, the angular distribution of high-energy photons can exhibit significant modifications due to QSE during the nlBW process. These modifications manifest as changes in divergence angles, either increasing or decreasing them. The observed asymmetry in the photon distribution provides a distinctive signature for identifying and quantifying the inherently stochastic nature of quantum processes governing photon behavior in intense laser fields. High-energy photons begin participating in the nlBW process after the LWFA electron beam interaction time $t = 5/\omega_L$. Due to QSE, the average divergence angle exhibits a bias, as shown in Fig. 7(e). The degree of photon involvement in the nlBW process can be inferred from changes in the average divergence angle. After the laser intensity peaks at $t = 6/\omega_L$, high-energy photons gradually decrease, a consequence of the stochastic nature of the process. The stages of high-energy photon participation in the nlBW process vary. As shown in Fig. 7(e), the average divergence angle of photons rapidly reaches its maximum within a single laser cycle, displaying a trend of maximum asymmetry, in contrast to Fig. 7(d). This subset of photons involved in the nlBW process generates a significant number of electron-positron pairs. Comparing Fig. 7(d) and Fig. 7(e), when colliding with a laser pulse of intensity $10^{22}\ \mathrm{W/cm^2}$, the peak of the average divergence angle occurs two laser cycles later than at $10^{23}\ \mathrm{W/cm^2}$. This indicates that as laser intensity increases, the nlBW process becomes more pronounced, and a longer effective laser pulse width is required for optimal colliding laser pulse selection. After the average divergence angle peaks, as photon energy is converted into positrons, the photon energy decreases, and the asymmetry diminishes due to the stochastic nature of the nlBW process. The probability of the nlBW process decreases, leading to a reduction in the slope of the evolution curve after the peak, as shown above. At the quantum level, the stochastic nature of the nlBW process implies that individual photons do not scatter or alter their properties in the presence of an electromagnetic field unless under extreme conditions, such as energies approaching the Schwinger limit or encountering exceptionally high field gradients where nonlinear QED effects dominate. Thus, the average photon angular distribution in the laser-plasma system, particularly for photons associated with LWFA electrons and nlBW positrons, reflects not only the initial laser characteristics but also the intricate interplay between the laser field, accelerated electrons, and the stochastic nature of QED processes. The stochasticity of photon emission and subsequent pair production introduces additional complexity to the kinetic description of electrons, making it essential to account for these effects in deflection angle analysis. Radiation reaction effects tend to narrow the energy distribution of electrons [42], while stochasticity broadens the momentum distribution. The combined action of Lorentz forces and QSE results in complex patterns in deflection angle distributions, which are crucial for understanding the transition from classical to quantum regimes.

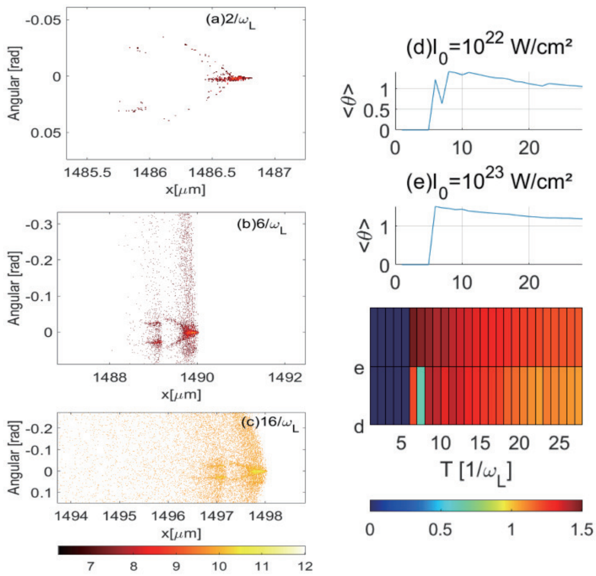

Fig. 7. Angular distribution of photons at interaction times $t = 2/\omega_{\mathrm{L}}$ (a), $t = 6/\omega_{\mathrm{L}}$ (b), and $t = 16/\omega_{\mathrm{L}}$ (c). The color scale represents $\log_{10}\left[\mathrm{d}^2N_e/\mathrm{d}\theta\mathrm{d}x\right]$ versus deflection angles $\theta = \arctan\left(p_y/p_x\right)$ and x-position. The evolution of the average divergence angle of photons during collisions at laser intensities of $10^{22}\ \mathrm{W/cm^2}$ (e) and $10^{23}\ \mathrm{W/cm^2}$ (f) reveals that, within a few interaction cycles, electrons efficiently transfer their energy to high-energy photons.

IV. CONCLUSION

In conclusion, our study investigates the significant role of quantum stochasticity effects (QSE) in the kinetic description of an LWFA electron beam colliding head-on with a linearly polarized laser pulse. The interplay between Lorentz forces and QSE gives rise to a rich combination of classical and quantum phenomena. Through detailed analysis of the angular distributions of the electron beam and resulting photons, we elucidate the characteristic evolution of both nonlinear Compton scattering (nlCS) and nonlinear Breit-Wheeler (nlBW) processes. This approach provides a practical method for examining a fundamental quantum property: the stochastic nature associated with the emission of high-energy photons and positrons.

The angular distribution of photons evolves over time, exhibiting clear signatures of QSE. The average divergence angle of photons shows a biased distribution, particularly in the high-energy regime, resulting from the complex interplay between the laser field and the stochastic nature of the nlBW process. Our findings highlight the importance of optimizing laser intensity and pulse width parameters, which enable comparative assessments of electron beam and photon divergence angle evolution. These adjustments are critical for enhancing the performance of LWFA-driven all-optical radiation sources and lepton pair production techniques.

By revealing these signals, our research provides empirical evidence essential for refining strategies in these areas. Such comparisons significantly improve our understanding and quantification of quantum stochasticity in these complex interactions, enriching the foundational knowledge of quantum phenomena. The findings offer valuable insights into the mechanisms governing these processes and underscore the need for advanced simulation techniques and theoretical frameworks to accurately model and predict particle behavior under extreme conditions.

---

[1] Berezhiani V I, Tskhakaya D D, Shukla P K.Pair production in a strong wake field driven by an intense short laser pulse[J].PhysicalReview A,1992,46(10). DOI:https://doi.org/10.1103/PhysRevA.46.6608.

[2] Podszus T, Dinu V, Piazza A D.Nonlinear Compton scattering and nonlinear Breit-Wheeler pair production including the damping of particle states[J].Physical review,D,2022,106(5). DOI:https://doi.org/10.1103/PhysRevD.106.056014

[3] Zamfir, N. V.Nuclear Physics with 10 PW laser beams at Extreme Light Infrastructure–Nuclear Physics (ELI-NP)[J].European Physical Journal Special Topics,2014,223(6). DOI:https://doi.org/10.1140/epjst/e2014-02176-0.

[4] Seipt D, Sorbo D D, Ridgers C P,et al.Theory of Radiative Electron Polarization in Strong Laser Fields[J].Physical Review A,2018. DOI:https://doi.org/10.1103/PhysRevA.98.023417.

[5] Wan F, Wang Y, Guo R T,et al.High-energy gamma-photon polarization in nonlinear Breit-Wheeler pair production and gamma-polarimetry[J]. 2020. DOI:https://doi.org/10.1103/PhysRevResearch.2.032049.

[6] Serov V D, Roshchupkin S P, Dubov V V.Resonant Effect for Breit–Wheeler Process in the Field of an X-ray Pulsar[J].Universe,2020, 6(11). DOI:https://doi.org/10.3390/universe6110190.

[7] Amsler, Claude, et al. "Pulsed production of antihydrogen." Communications Physics 4.1 (2021). DOI:https://doi.org/10.1038/s42005-020-00494-z

[8] Ji L L, Pukhov A, Nerush E N,et al.Near QED regime of laser interaction with overdense plasmas[J].European Physical Journal Special Topics,2014,223(6). DOI:https://doi.org/10.1140/epjst/e2014-02158-2.

[9] Poder K, Tamburini M, Sarri G,et al.Experimental Signatures of the Quantum Nature of Radiation Reaction in the Field of an Ultraintense Laser[J].Physical Review X,2018,8(3). DOI:https://doi.org/10.1103/PhysRevX.8.031004.

[10] Guo Z, Ji L, Yu Q,et al.Leveraging radiation reaction via laser-driven plasma fields[J].Plasma Physics and Controlled Fusion,2019,61(6). DOI:https://doi.org/10.1088/1361-6587/ab140b.

[11] Piazza D,A.First-order strong-field QED processes in a tightly focused laser beam[J].Phys.rev.a,2017,95(3). DOI:https://doi.org/10.1103/PhysRevA.95.032121.

[12] Vranic M, Grismayer T, Meuren S,et al.Are we ready to transfer optical light to gamma-rays?[J].Physics of Plasmas,2019, 26(5). DOI:https://doi.org/10.1063/1.5090992.

[13] Vranic M, Martins J L, Vieira J,et al.All-optical radiation reaction at 10^{21} W/cm^2.[J].Physical Review Letters,2014, 113(13). DOI:https://doi.org/10.1103/PhysRevLett.113.134801.

[14] Neitz N, Piazza A D.Stochasticity Effects in Quantum Radiation Reaction.2013. DOI:https://doi.org/10.1103/PhysRevLett.111.054802.

[15] Niel F, Riconda C, Amiranoff F,et al.From quantum to classical modeling of radiation reaction: A focus on stochasticity effects[J].Physical Review E,2018,97(4). DOI:https://doi.org/10.1103/PhysRevE.97.043209.

[16] Hu G, Sun W Q, Li B J,et al.Quantum-stochasticity-induced asymmetry in angular distribution of electrons in a quasi-classical regime[J].2020. DOI:https://doi.org/10.1103/PhysRevA.102.042218.

[17] Bula C, Mcdonald K T, Prebys E J.Observation of Nonlinear Effects in Compton Scattering[J].Physical Review Letters,1996,76(17). DOI:https://doi.org/10.1103/PhysRevLett.76.3116.

[18] Tajima T, Yan X Q, Ebisuzaki T.Wakefield acceleration[J].Reviews of Modern Plasma Physics,2020. DOI:https://doi.org/10.1007/s41614-020-0043-z.

[19] Shpakov V, Anania M P, Behtouei M,et al.First emittance measurement of the beam-driven plasma wakefield accelerated electron beam[J]. 2021. DOI:https://doi.org/10.1103/PhysRevAccelBeams.24.051301.

[20] Hue CS, Wan Y, Levine EY, Malka V. Control of electron beam current, charge, and energy spread using density downramp injection in laser wakefield accelerators. Matter and radiation at extremes.2023. DOI:https://doi.org/10.1063/5.0126293

[21] Jiang K, Wang W, Feng K, Li R. Review of Quality Optimization of Electron Beam Based on Laser Wakefield Acceleration. Photonics.2022,9(8). DOI:https://doi.org/10.3390/photonics9080511

[22] Lu W, Huang C, Zhou M,et al.Nonlinear Theory

for Relativistic Plasma Wakefields in the Blowout Regime[J].Physical ReviewLetters,2006,96(16). DOI:https://doi.org/10.1103/PhysRevLett.96.165002.

[23] Cole J M, Behm K T, Gerstmayr E,et al.Experimental observation of radiation reaction in the collision of a high-intensity laser pulse with a laser-wakefield accelerated electron beam[J].Phys.rev.x, 2018,8(1). DOI:https://doi.org/10.1103/PhysRevX.8.011020.

[24] Li X B, Qiao B, Liao Y L,et al.Possible signals in differentiating the quantum radiation reaction from the classical one[J].2020. DOI:https://doi.org/10.1103/PhysRevA.101.032108.

[25] Li Y F, Zhao Y T, Hatsagortsyan K Z,et al.Electron-angular-distribution reshaping in the quantum radiation-dominated regime[J].Physical Review A. DOI:https://doi.org/10.1103/PhysRevA.98.052120.

[26] Nerush E N,et al.Laser Field Absorption in Self-Generated Electron-Positron Pair Plasma[J] Phys. Rev. Lett.2011, 106, 035001.DOI:https://doi.org/10.1103/PhysRevLett.106.109902.

[27] Tamburini M , Meuren S .Efficient high-energy photon production in the supercritical QED regime[J].American Physical Society (APS), 2021.DOI:https://doi.org/10.1103/PhysRevD.104.L091903.

[28] Ritus V I.Quantum effects of the interaction of elementary particles with an intense electromagnetic field[J].Journal of Soviet Laser Research,1985,6(5). DOI:https://doi.org/10.1007/BF01120220.

[29] Sokolov A A, Ternov I M, Bagrov V G,et al.Radiation-induced self-polarization of the electron spin for helical motion in a magnetic field[J].Soviet Physics Journal,1968,11(5). DOI:https://doi.org/10.1007/BF00816590.

[30] Di Piazza A ,Müller, C, Hatsagortsyan K Z ,et al.Extremely high-intensity laser interactions with fundamental quantum systems[J].Review of Modern Physics,2011,84(3). DOI:https://doi.org/10.1103/revmodphys.84.1177.

[31] Bell A R, Kirk J G.Possibility of Prolific Pair Production with High-Power Lasers[J].Physical Review Letters,2008,101(20). DOI:https://doi.org/10.1103/PhysRevLett.101.200403.

[32] Blackburn T, Ilderton A, Murphy C D,et al.Scaling laws for positron production in laser-electron-beam collisions[J].American Physical Society,2017. DOI:https://doi.org/10.1103/PHYSREVA.96.022128.

[33] King B.Interference effects in nonlinear Compton scattering due to pulse envelope[J].Physical Review D,2021. DOI:https://doi.org/10.1103/PhysRevD.103.036018.

[34] Blackburn,T,G,et al.Nonlinear Breit-Wheeler pair creation with bremsstrahlung gamma rays[J].Plasma physics and controlled fusion,2018. DOI:https://doi.org/10.1088/1361-6587/aab3b4.

[35] Golub A,S. Villalba-Chávez, Ruhl H,et al.Linear Breit-Wheeler pair production by high-energy bremsstrahlung photons colliding with an intense x-ray laser pulse[J].Physical Review D,2021(1). DOI:https://doi.org/10.1103/PHYSREVD.103.016009.

[36] Jansen M J A ,Kamiński, J. Z, Krajewska K ,et al.Strong-field Breit-Wheeler pair production in short laser pulses: Relevance of spin effects[J].2016. DOI:https://doi.org/10.48550/arXiv.1605.03476.

[37] Ridgers C P ,et al.Modelling gamma-ray photon emission and pair production in high-intensity laser–matter interactions[J].Journal of Computational Physics, 2014, 260(1):273-285.DOI:https://doi.org/10.1016/j.jcp.2013.12.007.

[38] Duclous R , Kirk J G , Bell A R .Monte Carlo calculations of pair production in high-intensity laser–plasma interactions[J].IOP Publishing, 2011(1).DOI:https://doi.org/10.1088/0741-3335/53/1/015009.

[39] Arber T D,et al.Contemporary particle-in-cell approach to laser-plasma modelling[J].2015.DOI:https://doi.org/10.1088/0741-3335/57/11/113001.

[40] Fedotov A M , Narozhny N B , Mourou G ,et al.Limitations on the attainable intensity of high power lasers[J].Physical Review Letters, 2010, 105(8):080402. DOI:https://doi.org/10.1103/PhysRevLett.105.080402.

[41] [1] Vranic M , Grismayer T , Fonseca R A ,et al.quantum radiation reaction in head-on laser-electron beam interaction[J].new journal of physics, 2016.DOI:https://doi.org/10.1088/1367-2630/18/7/073035.

[42] Tamburini M, Pegoraro F, Piazza A D,et al.Radiation reaction effects on radiation pressure acceleration[J].New Journal of Physics,2010,12(12). DOI:https://doi.org/10.1088/1367-2630/12/12/123005.